

**Infrared Spectroscopy with a Cavity Ring-Down  
Spectrometer**

**by Logan S Marcus, Ellen L Holthoff, and Paul M Pellegrino**

**ARL-TR-7031**

**August 2014**

## **NOTICES**

### **Disclaimers**

The findings in this report are not to be construed as an official Department of the Army position unless so designated by other authorized documents.

Citation of manufacturer's or trade names does not constitute an official endorsement or approval of the use thereof.

Destroy this report when it is no longer needed. Do not return it to the originator.

**Army Research Laboratory**

Adelphi, MD 20783-1138

---

---

**ARL-TR-7031**

**August 2014**

---

**Infrared Spectroscopy with a Cavity Ring-Down  
Spectrometer**

**Logan S Marcus, Ellen L Holthoff, and Paul M Pellegrino**  
**Sensors and Electron Devices Directorate, ARL**

# REPORT DOCUMENTATION PAGE

*Form Approved*  
OMB No. 0704-0188

Public reporting burden for this collection of information is estimated to average 1 hour per response, including the time for reviewing instructions, searching existing data sources, gathering and maintaining the data needed, and completing and reviewing the collection information. Send comments regarding this burden estimate or any other aspect of this collection of information, including suggestions for reducing the burden, to Department of Defense, Washington Headquarters Services, Directorate for Information Operations and Reports (0704-0188), 1215 Jefferson Davis Highway, Suite 1204, Arlington, VA 22202-4302. Respondents should be aware that notwithstanding any other provision of law, no person shall be subject to any penalty for failing to comply with a collection of information if it does not display a currently valid OMB control number.

**PLEASE DO NOT RETURN YOUR FORM TO THE ABOVE ADDRESS.**

<b>1. REPORT DATE (DD-MM-YYYY)</b> August 2014	<b>2. REPORT TYPE</b> Final	<b>3. DATES COVERED (From - To)</b> 01/2013–07/2014	
<b>4. TITLE AND SUBTITLE</b> Infrared Spectroscopy with a Cavity Ring-Down Spectrometer		<b>5a. CONTRACT NUMBER</b> W911NF-12-2-0019	
		<b>5b. GRANT NUMBER</b>	
		<b>5c. PROGRAM ELEMENT NUMBER</b>	
<b>6. AUTHOR(S)</b> Logan S Marcus, Ellen L Holthoff, and Paul M Pellegrino		<b>5d. PROJECT NUMBER</b>	
		<b>5e. TASK NUMBER</b>	
		<b>5f. WORK UNIT NUMBER</b>	
<b>7. PERFORMING ORGANIZATION NAME(S) AND ADDRESS(ES)</b> U.S. Army Research Laboratory ATTN: RDRL-SEE-E 2800 Powder Mill Road Adelphi, MD 20783-1138		<b>8. PERFORMING ORGANIZATION REPORT NUMBER</b>  ARL-TR-7031	
<b>9. SPONSORING/MONITORING AGENCY NAME(S) AND ADDRESS(ES)</b>		<b>10. SPONSOR/MONITOR'S ACRONYM(S)</b>	
		<b>11. SPONSOR/MONITOR'S REPORT NUMBER(S)</b>	
<b>12. DISTRIBUTION/AVAILABILITY STATEMENT</b> Approved for public release; distribution unlimited.			
<b>13. SUPPLEMENTARY NOTES</b>			
<b>14. ABSTRACT</b> There is a pressing need for airborne hazard detectors for both Army and civilian use. Cavity ring-down spectroscopy (CRDS) is a capable and sensitive detection method for hazardous materials that is based on the principles of electromagnetic radiation spectroscopy. Research has been ongoing at the US Army Research Laboratory (ARL) to evaluate the sensitivity and limitations of two commercial CRDSs. These devices were manufactured by Los Gatos Research, Inc., and provided to ARL via collaboration with the Edgewood Chemical Biological Center (ECBC). Evaluation of the spectrometers comprises background noise determination, spectroscopic confirmation, and limit of detection testing. At each step, the CRDSs proved to be accurate and sensitive apparatus.			
<b>15. SUBJECT TERMS</b> Cavity ring down, infrared spectroscopy, hazard detection, ammonia, 1,4-dioxane			
<b>16. SECURITY CLASSIFICATION OF:</b>			<b>17. LIMITATION OF ABSTRACT</b>  UU
<b>a. REPORT</b> Unclassified	<b>b. ABSTRACT</b> Unclassified	<b>c. THIS PAGE</b> Unclassified	
			<b>18. NUMBER OF PAGES</b>  42
<b>19a. NAME OF RESPONSIBLE PERSON</b> Logan S Marcus			
			<b>19b. TELEPHONE NUMBER (Include area code)</b> 301-394-2564

---

## Contents

---

<b>List of Figures</b>	<b>iv</b>
<b>Acknowledgments</b>	<b>v</b>
<b>1. Introduction</b>	<b>1</b>
1.1 Hazard Detection .....	1
1.2 Origins .....	1
1.3 Cavity Ring-Down Spectrometer .....	2
<b>2. Experimental Setup</b>	<b>5</b>
2.1 Device.....	5
2.2 Laboratory Setup .....	6
2.3 Computer Control and Data Analysis .....	7
<b>3. Experimental Results</b>	<b>8</b>
3.1 Nitrogen.....	8
3.2 Ammonia.....	9
3.3 1,4-Dioxane .....	13
<b>4. Literature Comparison</b>	<b>17</b>
4.1 Public Databases.....	17
4.2 Ammonia.....	17
4.3 1,4-Dioxane .....	21
4.4 ARL Experimental Data Comparison .....	25
<b>5. Conclusions</b>	<b>27</b>
<b>6. References</b>	<b>29</b>
<b>List of Symbols, Abbreviations, and Acronyms</b>	<b>31</b>
<b>Distribution List</b>	<b>33</b>

---

## List of Figures

---

Fig. 1	Diagram of the exponential decay of the PMT response as a function of time for a theoretical CRDS experiment <sup>2</sup> .....	4
Fig. 2	Schematic diagram of the CRDS system under investigation. The schematic is not to scale and omits several components for clarity and visibility. <sup>10</sup> .....	5
Fig. 3	Photograph of the inside of the CRDS system. The laser head is the blue and white box on the far left of the device. The detector is the red cylinder with a gold top in the upper right-hand corner. The cavity is the orange wrapped cylinder at the top of the unit. Other major components are the laser controller underneath the data acquisition hardware on the bottom right, and the computer in front and in the middle. ....	6
Fig. 4	Plot of measured loss vs. excitation laser wavelength for nitrogen. This plot details the background signal measured by the spectrometer because nitrogen gas has no infrared absorption in the studied wavenumber range. The background is a combination of the variations in excitation laser power and other experimental factors.....	9
Fig. 5	Plot of measured loss vs. excitation laser wavelength for the ammonia gas sample .....	10
Fig. 6	Plot of measured loss vs. excitation wavenumber for 10 ammonia concentrations .....	11
Fig. 7	Plot of measured ammonia absorption vs. concentration at one of the absorption maxima ( $930\text{ cm}^{-1}$ ) .....	12
Fig. 8	Plot of loss vs. wavenumber for highest used concentration of 1,4-dioxane .....	14
Fig. 9	Measured loss vs. excitation wavenumber for multiple 1,4-dioxane concentrations .....	15
Fig. 10	Measured loss vs. 1,4-dioxane concentration .....	16
Fig. 11	Ammonia spectrum from PNNL .....	18
Fig. 12	Comparison between CRDS (blue) and PNNL (red) absorption spectra for ammonia....	19
Fig. 13	Comparison of ammonia spectra from NIST (top) and CRDS (bottom). The letters A through H denote spectral features used for comparison between the four spectra .....	20
Fig. 14	1,4-dioxane spectrum from PNNL .....	22
Fig. 15	Comparison between PNNL (blue) and CRDS (red) spectra for 1,4-dioxane .....	23
Fig. 16	Comparison between NIST reference data (top) and CRDS experimental data (bottom). The two spectra in the top plot have different data sources and sensitivities. ....	24
Fig. 17	Comparison of the three spectroscopic methods. The two CRDS spectra (green and black) are compared to FTIR (red) and PAS (blue).....	26

---

## **Acknowledgments**

---

We would like to thank Alan Samuels and Erin Davis from the US Army Edgewood Chemical Biological Center (ECBC) for providing the spectrometers and other technical advice during this investigation.

This work was supported in part by an appointment to the US Army Research Laboratory (ARL) Postdoctoral Fellowship Program administered by the Oak Ridge Associated Universities (ORAU) through a contract with ARL.

INTENTIONALLY LEFT BLANK.

---

# 1. Introduction

---

## 1.1 Hazard Detection

The Army's constant need for hazardous chemical safety drives critical research into the detection of airborne threats. Various electromagnetic radiation spectroscopy methods have proven to be well suited to the task of detecting trace amounts of battlefield-relevant threats.<sup>1-3</sup> These methodologies rely on the fact that each chemical species has a unique absorption response when exposed to monochromatic light. Each spectroscopic method involves the absorption of radiation and the measurement of the resultant system change.

In photoacoustic spectroscopy (PAS), the resultant system change measured is a pressure wave generated by modulating the excitation source.<sup>1</sup> Fourier transform infrared spectroscopy (FTIR) measures the transmission of the excitation source and then calculates the absorption from that measured transmission.<sup>3</sup> Cavity ring-down spectroscopy (CRDS) measures the decay of a single laser pulse between two highly reflective mirrors.<sup>2</sup> The pulse decay as a function of time is relatable to the absorption coefficient of whatever gaseous medium the laser pulse traverses between the mirrors.<sup>2</sup> Once absorption is determined through the desired measurement technique, the identification of the analyte is a matter of matching spectral features.<sup>4</sup>

## 1.2 Origins

In laser absorption spectroscopy for dilute gases in the limit of weak absorption, there is a linear relationship between the measured signal and the path length traveled by an excitation source.<sup>5</sup> Maximization of weak signals is, and was, the goal of much spectroscopic research as the identification of trace constituents of various samples provides a wealth of information. Hazardous chemical detection also values signal maximization for improved limits of detection. Earlier techniques used a multipass optical cell to increase the interaction path length of the analyte and the excitation source from the physical size of the sample chamber to a virtual size on the order of several hundred meters.<sup>5</sup> This is labeled a virtual increase in sample interaction length, because the excitation source travels a virtual length, bouncing between two highly reflective mirrors, beyond the capacity of the actual chamber.

It was with signal maximization in mind that CRDS emerged from techniques developed to measure the reflectivity of mirrors.<sup>2</sup> CRDS improved the sensitivity of the preceding multipass techniques by using tunable pulsed lasers as the excitation source.<sup>5</sup> The mirrors at either end of the chamber transmit a known fraction of the pulsed beam. Increases in sensitivity are accomplished by measuring the time rate of change of the intensity of the fraction of light that is transmitted through the highly reflective mirrors that terminate each end of the chamber.<sup>5</sup> The sensitivity of this measurement technique increases as sample absorption decreases, leading to higher sensitivity at the lower analyte concentrations.<sup>5</sup> The general principles on the construction

of a CRDS were developed in the late 1980s, but their modern counterparts have stayed close to the original design.<sup>6,7</sup>

### 1.3 Cavity Ring-Down Spectrometer

As with other spectroscopic methodologies, a CRDS is constructed from three key components: a sample chamber, an excitation source, and a detection device. For CRDS, the sample chamber does more than hold the gaseous sample under investigation. The chamber is a cylindrical cavity that is capped at both ends by highly reflective mirrors that allow for a pulse of light to bounce back and forth so often that a 1-m length of cavity can simulate a cavity on the order of 10 km long. The interaction path length is one of the most important features of the method; path length being directly related to sensitivity. The simulated length of the CRDS cavity is calculated by multiplying twice the cavity length by the number of round trips,  $n$ , before the intensity of the laser pulse falls to  $1/e$  of the starting intensity. The number of round trips can be expressed as a function of the reflectivity of the end mirrors  $R$ :<sup>2</sup>

$$n = \frac{-1}{2\ln(R)}. \quad (1)$$

For example, a 1-m-long cavity bound by mirrors of reflectivity 0.9999 would have an  $n$  value of 5000 corresponding to a simulated length of 10 km. The mirrors and mirror coatings are selected for particular wavelength ranges so that they can provide the maximum reflectance and increase the background path length calculated in Eq. 1.<sup>2</sup> The analyte under investigation dictates the wavelength range for the mirrors and the excitation source. In most CRDS applications, the excitation source is a pulsed tunable laser, often in the infrared range.

The cavity used in CRDS offers an advantage over other traditional absorption spectroscopy methods. In gaseous PAS, the excitation laser has a very short interaction path through the analyte. This short interaction path limits the amount of excitation radiation that can be absorbed because there is an exponentially decreasing relation between fraction of absorbed light,  $(I/I_0)$ , and the path the light travels,  $l$ . The absorption coefficient  $\alpha$  is a constant that varies based on analyte and excitation source wavelength. This relationship is the Beer-Lambert law that describes electromagnetic radiation spectroscopy:

$$\frac{I}{I_0} = e^{-\alpha l}. \quad (2)$$

We can take Beer-Lambert and express the fraction of transmitted light  $(I/I_0)$  on the left-hand side of Eq. 2 as a function of time. This expression is important for analyzing the digital signal generated in a CRDS experiment. The fraction of transmitted light can be generalized in terms of the number,  $n$ , of round trips between the two mirrors with reflectivity,  $R$ :<sup>8</sup>

$$\frac{I}{I_0} = \{Re^{-\alpha l}\}^{2n}. \quad (3)$$

Because energy must be conserved, we know that the total reflected light must sum to unity with the transmitted fraction and the losses from diffraction and Rayleigh scattering. This allows us to write the fraction of transmitted light as

$$\frac{I}{I_0} = e^{-2n(L+T+\alpha l)}, \quad (4)$$

where  $L$  is the loss factor for the end mirrors and  $T$  is the fraction of transmitted light through the mirrors. We know that the time it takes a pulse of laser light to traverse the cavity can be calculated by dividing the length of the cavity by the speed of light. Multiplying that quotient by twice the number of round trips allows for the replacement of the discrete  $n$  with the continuous  $t$ :

$$\frac{I(t)}{I_0} = e^{-\frac{ct}{l}(L+T+\alpha l)}. \quad (5)$$

Grouping the terms in the exponential of Eq. 5 and defining the empty cavity decay time,  $\tau$ , as  $\tau=l/c(T+L)$  allows for the simplification of Eq. 5 into<sup>8</sup>

$$\frac{I(t)}{I_0} = e^{-\left(\frac{t}{\tau} + \alpha ct\right)}. \quad (6)$$

The two terms in the exponential are the time-dependant decay of the initial laser pulse due to the constant experimental parameters on the left and the analyte-dependant decay of the pulse that is dependent on the absorption coefficient on the right. The modified Beer-Lambert law in Eq. 6 is used in the numerical analysis of data collected by the CRDS.

The detection device for CRDS is commonly a photomultiplier tube (PMT) or a photovoltaic detector (PVD) placed behind the mirror at the opposite end of the cavity from the injection point of the excitation source. A PMT works by measuring the chain reaction of the cascading electron emission from the photoemissive surfaces when a photon is incident on the collection window.<sup>3</sup> A PVD device generates an electrical signal when a photon of sufficient energy promotes an electron from the valence band to the conduction band.<sup>9</sup> The detector in a CRDS collects the small percentage of photons that are transmitted through the mirrors capping the cavity. The number of transmitted photons decreases as the excitation pulse bounces between the mirrors due to molecular absorption, diffraction, Rayleigh scattering, and other dissipative effects. The decrease caused by cavity losses is a source of constant loss, and molecular absorption of the pulse by the contents of the cell varies based on the molecular composition of the interstitial gas. The electrical output from the detector is recorded as a function of time, aided by a computer, and fit with an exponentially decaying function. Figure 1 is a diagram of PMT response versus time for a theoretical CRDS experiment.<sup>2</sup> The theoretical response of a PVD detector will look the same, and though there are experimental reasons to choose one detection method over the other, they are not discussed here.

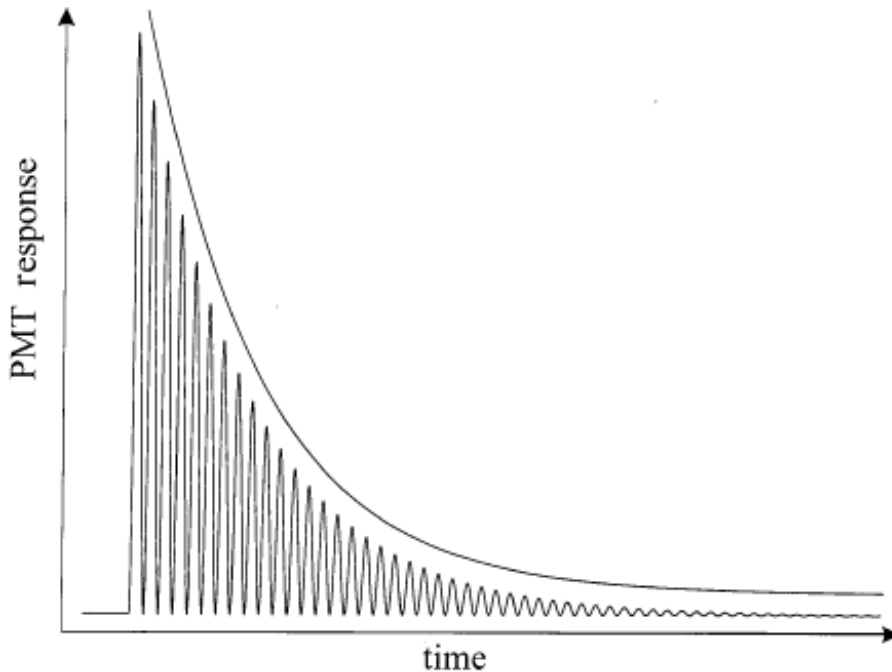


Fig. 1 Diagram of the exponential decay of the PMT response as a function of time for a theoretical CRDS experiment<sup>2</sup>

The digitized signal produced by the detector is recorded as a function of time and is analyzed by determining the first-order decay constant for every pulse.<sup>2</sup> This decay constant is a function of the experimental setup and the absorption coefficient of the gas in the cavity, and can be compared to the contents of the exponential in Eq. 6. The experimental setup remains constant throughout the experiment and thus the absorption coefficient is directly calculable from the decay constant. This calculation is accomplished by comparing the change in decay constants between a non-reactive analyte, nitrogen gas, for example, and an analyte known to be active in the wavelength range of the excitation source.

Every CRDS system is unique and can differ in large or small ways. The experimental setups vary from the length of the cavity to the software that analyzes the output from the detector. The experimental setups also vary based upon the goals for the detector; however, the guiding principles of analysis and experimental design remain constant. A CRDS system measures the decay rates of a monochromatic pulse of light and uses that decay to extrapolate information about the contents of the cavity. The work discussed in this report was accomplished using a set of two CRDSs. The analysis of the CRDS method discussed herein can be extended to the general case despite that specificity.

---

## 2. Experimental Setup

---

### 2.1 Device

The evaluated devices are a pair of CRDSs built for the US Army Edgewood Chemical Biological Center (ECBC) by Los Gatos Research, Inc. (LGR),<sup>10</sup> via an Army Small Business Innovation Research (SBIR) Phase II program. The devices are very similar to the generic CRDS devices discussed in Section 1.3 and are almost completely self-contained, requiring very little in the way of laboratory support for their operation. The CRDS sensors come preloaded with the required analytical software to fit the measured pulse decay curves and remove the constant background features from the data. Both sensors share the vast majority of their components, the notable exception being the excitation source, therefore the configuration of only one of the sensors is discussed in detail.

A schematic of the CRDS system from LGR is depicted in Fig. 2.<sup>10</sup> The schematic is not drawn to scale and the placement of the components has been optimized for visibility, not for the best representation of the actual system. The diagram depicts the major components of the system that were discussed in Section 1.3 and most of the important supporting parts. The cavity is a stainless steel cylinder that is capped at both ends by high reflectance mirrors. There are two sensors, one for pressure and one for temperature, to monitor the inner conditions of the cavity. The cavity was designed for gaseous samples and has two valves to control gas flow into, through, and out of the cavity.

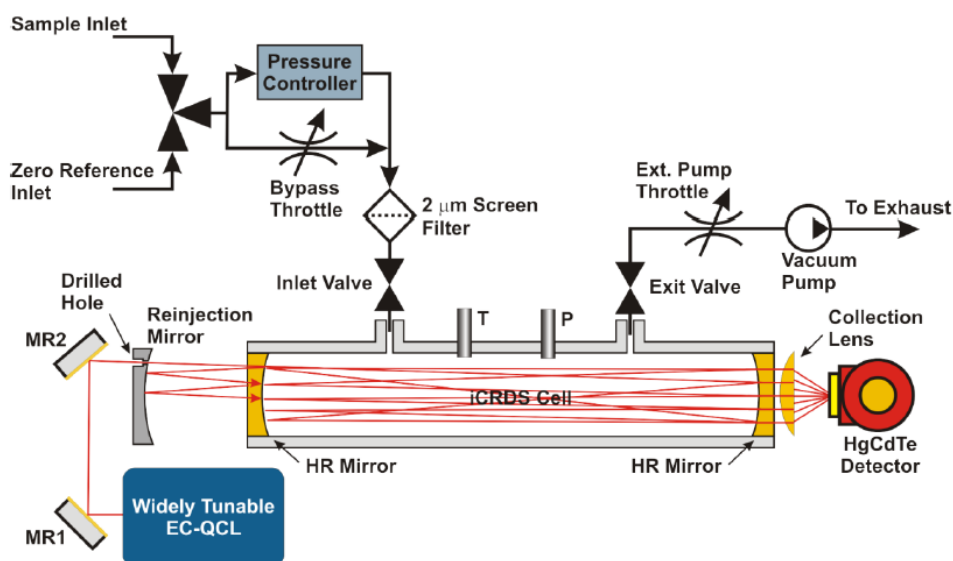


Fig. 2 Schematic diagram of the CRDS system under investigation. The schematic is not to scale and omits several components for clarity and visibility.<sup>10</sup>

The excitation source for the CRDS system is a quantum cascade laser (QCL) that is wavelength tunable in the infrared region. The laser, produced by Daylight Solutions, Inc.,<sup>11</sup> is a tunable pulsed external cavity quantum cascade laser (ECQCL) and is available commercially. The ECQCLs produced by Daylight are available in a variety of center wavelengths for a collective tuning range of about 4–12  $\mu\text{m}$  or about 830–2500  $\text{cm}^{-1}$ . The two ECQCLs used in the CRDS systems have wavenumber ranges of 820–1000 and 1000–1200  $\text{cm}^{-1}$ .

Mercury, cadmium, and tellurium (HgCdTe) combined form a PVD capable of measuring the fraction of infrared light that is transmitted through the highly reflective mirror at the end of the CRDS cavity. The HgCdTe detector must be cooled with liquid nitrogen to minimize detector noise and minimize the detection threshold. The photograph of the interior of the detector (Fig. 3) shows many more parts than seen in Fig. 2. Most notably, the laser controller at the far right, the data acquisition hardware on top of the laser controller, and the guts of a laboratory personal computer, which can be seen beneath the central processing unit (CPU) fan on the motherboard in the middle of the photograph.



Fig. 3 Photograph of the inside of the CRDS system. The laser head is the blue and white box on the far left of the device. The detector is the red cylinder with a gold top in the upper right-hand corner. The cavity is the orange wrapped cylinder at the top of the unit. Other major components are the laser controller underneath the data acquisition hardware on the bottom right, and the computer in front and in the middle.

## 2.2 Laboratory Setup

The CRDS devices arrived from LGR almost ready for data acquisition. The laser head needed to be mounted and aligned, the computer in the instruments needed standard peripherals (e.g., a mouse, keyboard, and monitor), and the devices needed an analyte delivery system. Analyte control is perhaps the most important experimental control required for qualitative and quantitative analysis and safety. Strict regulation of the sample concentration reduces a major factor in experimental uncertainty, and proper ventilation reduces the hazards involved in studying analytes that have particular interest for the Army.

The implemented solution for analyte control used in this analysis is an Owlstone OVG-4 calibration gas generator from Owlstone Nanotech, Inc., and permeation tubes.<sup>12</sup> Permeation tubes are a calibrated combination of fluid analyte encased in a polymer that, when heated to a specific temperature, emit a precise amount of the analyte in a gaseous state. This gaseous emission can be combined with a flow of a carrier gas (e.g., nitrogen gas) producing a constant flow with a known concentration of the analyte. The known concentration of the analyte is a function of the permeation tube, temperature, analyte composition, and nitrogen gas flow. The first three factors are constants for each permeation tube. The nitrogen gas flow is a tunable factor allowing for variation in the analyte concentration. The CRDS system has built-in computer-controlled sample flow valves and requires connections only to the calibration gas generator and exhaust.

### **2.3 Computer Control and Data Analysis**

Each CRDS device has its own built-in computer for data acquisition and experimental control. The computers came preloaded with the necessary software to control the spectrometer and collect data. The computer inside the spectrometer is a desktop computer without a case, running full versions of Microsoft Windows<sup>®</sup> and LabVIEW software. The manufacturer of the spectrometers has developed and included LabVIEW programs with graphical interfaces for the operation of the spectrometers and data analysis, though the data analysis software was eschewed for the more familiar Microsoft Excel for the work described herein.

The experimental parameters under computer control are the inlet and outlet valves for the cavity, the excitation laser, and the PVD. Inlet and outlet valves control sample flow through the cavity. Computer control of several laser parameters is important for data collection and processing. For data collection, the PVD generates the highest signal-to-noise ratio (SNR) when the initial energy of the excitation laser pulse is highest. This is the case because the spectrometer measures the decay pattern of a single laser pulse that has been attenuated by environmental factors in addition to analyte molecular absorption. Maximization of the initial laser power will maximize the number of measureable round trips of the pulse and allow the software to generate the most accurate fit for the data.

Additionally, computer control of the laser allows for automation of the data collection process. Simplified acquisition of data involves measuring the ring-down time at a constant analyte concentration at every wavelength in the tuning range of the excitation source. Having the computer control the output wavelength of the excitation laser and the collection of data enables the desired automation.

Computer control of the experiment and data handling streamlines the data and experimental analysis procedures. The exponential decay of the excitation pulse was numerically described in Eq. 6, and in that equation, the pulse decay depended on two factors, one being the desired molecular absorption of the analyte being investigated. The other factor was a constant that depended on the experimental parameters; that constant can be measured for a set experimental

setup and then erased from the data leaving only the desired information about the analyte. This background removal is discussed further in Section 3. The output from the spectrometers is a generic data file that can be imported into Microsoft Excel for analysis.

---

### 3. Experimental Results

---

#### 3.1 Nitrogen

The production of the calibrated analytes uses nitrogen gas flowing over the emitting permeation tube. Nitrogen gas is used because it is relatively inert, not active in the infrared region, and prevalent in air. The lack of reactivity aids in the study of the analyte, making sure that the measured response is that of the desired analyte only and not specific to a reaction with the carrier gas. The excitation laser does not have a flat power output versus wavelength relationship. The laser has highest power at the center wavelength and decreasing power as the wavelength moves away from that value. Because of this, any measurement that is dependent on the power of the laser, spectroscopy being one, must account for the excitation laser power variation. Nitrogen being inactive in the wavelength range of the excitation laser enables the measurement of the laser power curve for changing wavelength, and thus, the elimination of diminishing power's effect on the measured spectrum. Nitrogen is also a natural choice for evaluation of any sensor that has a future application in chemical sensing. Nitrogen gas is the most abundant component, about 78% of air. If the spectrometer does not function with nitrogen as the carrier gas, it will have a much harder time working in any practical environment.

The first series of measurements taken with either spectrometer are nitrogen backgrounds. Pure nitrogen gas flows through the cavity and a scan over wavelength is performed. Figure 4 is a plot of loss versus excitation laser wavenumber. The software takes the exponential ring-down measured by the photodetector and calculates a value that is directly proportional to the absorption of whatever is in the cavity. For the purpose of this report, the value measured by the spectrometer is called *loss* and is recorded in arbitrary units (A.U.). Because nitrogen has no infrared absorption feature, the measured background in Fig. 4 is the background noise that is in the system. The background is a combination of varying laser power and experimental noise sources. This measured background can be subtracted from spectra measured with an absorbing analyte to isolate the infrared spectrum of the analyte.

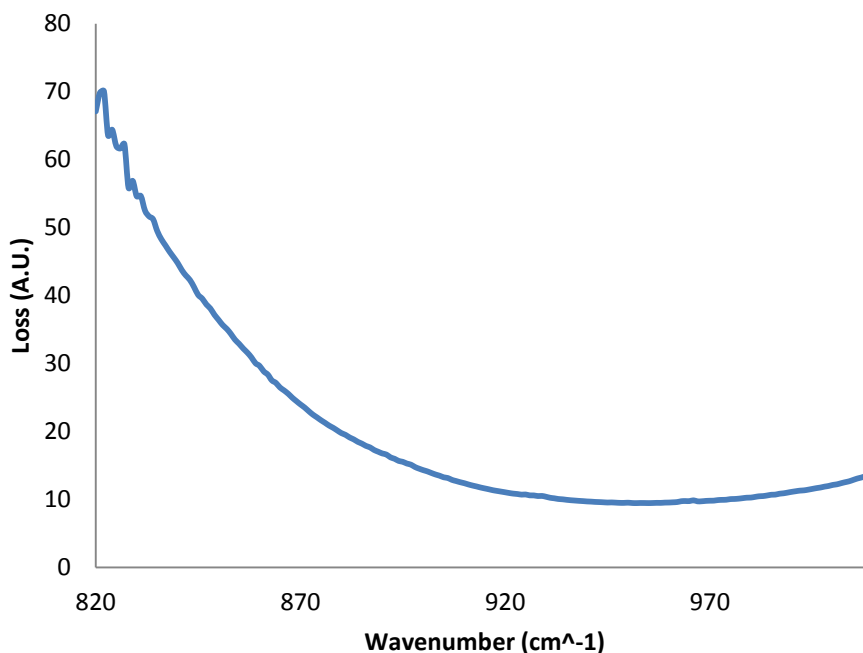


Fig. 4 Plot of measured loss vs. excitation laser wavelength for nitrogen. This plot details the background signal measured by the spectrometer because nitrogen gas has no infrared absorption in the studied wavenumber range. The background is a combination of the variations in excitation laser power and other experimental factors.

The experimental factors that contribute to the background seen in Fig. 4 can fluctuate slightly over time and therefore an average of several background measurements was taken and used as the baseline for the data analysis of the selected analytes. This average also aids in the calculation of the noise floor of the system. The noise floor changes with respect to wavenumber and that causes the minimum detectable signal to vary depending on the analyte because different analytes have absorption features at different wavenumbers. Because the minimum detectable limits vary by analyte, the specific wavenumbers for each are discussed with their experimental results later in this report. It is important to note that there is a lot of noise in the lower wavenumber section of the plot. Above  $840\text{ cm}^{-1}$ , the loss spectrum is smooth and consistent, which lowers the standard deviation of the background, which is very important in attaining the smallest possible detectable limit. This noise varies across different background spectra and likely is the result of low excitation laser power at the extremes of the power spectrum.

### 3.2 Ammonia

The first analyte investigated in the evaluation of the CRDSs was ammonia. Ammonia was chosen for two main reasons. The first being that it has absorption peaks in the tuning range of the excitation laser in one of the spectrometers ( $820\text{ to }1010\text{ cm}^{-1}$  or  $9.8\text{ to }12.2\text{ }\mu\text{m}$ ). This is a binary condition, either the absorption feature of the molecule is appropriate or it is unusable for

evaluation. The second reason why ammonia was selected is because the overarching goal of this work is studying hazard detection. Ammonia is classified as a high hazard toxic industrial chemical (TIC) by the Occupational Safety and Health Administration,<sup>13</sup> and therefore, ammonia detection is a practical and useful application for a gas sensor.

A high concentration of ammonia is used for initial detection studies because a higher concentration of analyte generally results in a larger sensor response. This occurs by increasing the number of absorbers in the path of the excitation laser, which, in turn, decreases the effective path length experienced by the excitation laser by increasing the number of possible absorption sites. The relationship between sample concentration and measured CRDS signal is used later for a quantitative evaluation of the detector. For now, the high concentration of the analyte is used to increase the qualitative investigation into the performance of the spectrometer by magnifying subtle features that might not be visible or differentiable at lower concentrations and signal levels. Figure 5 is a plot of the measured loss versus excitation laser wavenumber.

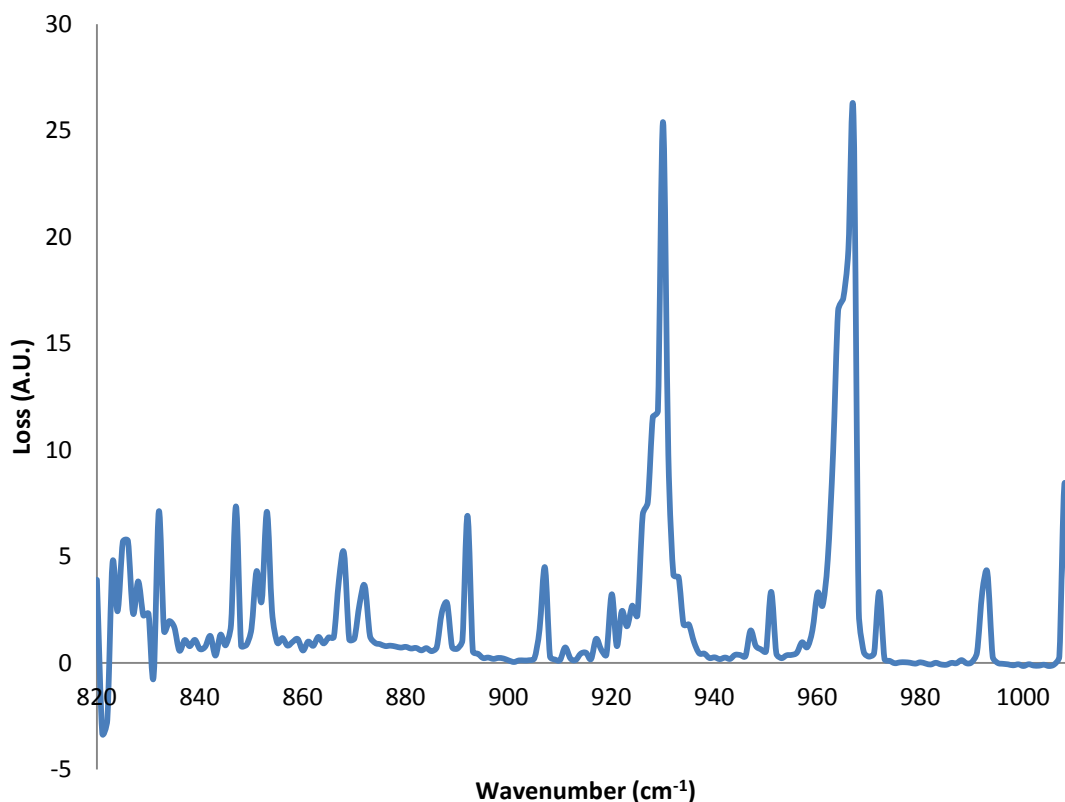


Fig. 5 Plot of measured loss vs. excitation laser wavelength for the ammonia gas sample

The low wavenumber negative loss values are artifacts of the background variation in the lower power region of the spectrum. The measured loss at the extreme lower end of the wavenumber spectrum, seen in Fig. 4, is so close to zero that small variance is enough to shift the ammonia spectrum negative when the averaged background is subtracted from the raw signal data. The

two main absorption peaks are at  $930$  and  $967\text{ cm}^{-1}$ , and they are the focus of the ammonia limits of detection work. The low absorption doublets between  $900$  and  $840\text{ cm}^{-1}$  are discussed by McKean and Schatz, and are an excellent check on the qualitative accuracy of the spectrum.<sup>14</sup>

Calculation of the limit of detection for ammonia starts with recording the absorption spectrum at a wide range of analyte concentrations. Figure 6 is a plot of the group of spectra taken for ammonia at concentrations between  $4.6\text{ ppm}$  and  $460\text{ ppb}$ .

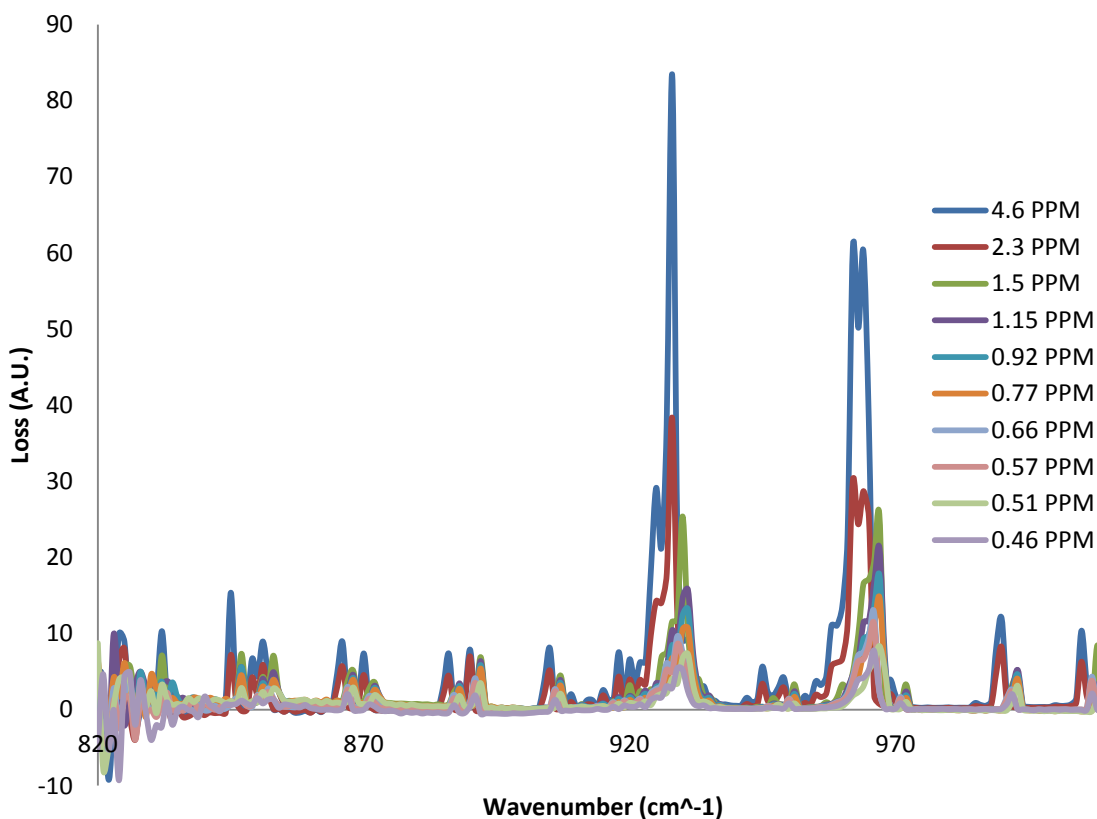


Fig. 6 Plot of measured loss vs. excitation wavenumber for 10 ammonia concentrations

There is a clear relationship between the quantity of ammonia in the spectrometer and the measured loss, evidenced by the decreasing loss measured as the concentration decreases. This is logical because increasing the amount of ammonia increases the number of possible absorbers for the excitation laser and thus decreases the number of reflections the pulse can make before being fully attenuated. This relationship is the basis for determining the sensitivity of the detector. The varied spectra are not, however, perfect copies of each other. It is important to note that there is a discernible shift in peak wavenumber as the concentration of ammonia decreases. The highest two concentration values ( $4.6$  and  $2.3\text{ ppm}$ ) both have their peak absorption values shifted between  $2$  and  $3\text{ cm}^{-1}$ . We believe that this shift arises from clumping of the ammonia due to the higher concentration values. This shift in absorption features and the forming of dimers and trimers in ammonia have been discussed previously in the literature.<sup>15,16</sup> It is because

of that shift that we examined the 1.5-ppm absorption spectrum in Fig. 5, and why we use the 1.5-ppm data for external comparison in section 3.3.

A plot of the measured loss versus ammonia concentration (Fig. 7) can be constructed using the lower of the two absorption peaks as the fixed comparison point. This plot examines the relationship between those two factors. This relationship is then used to determine the sensitivity of the instrument.

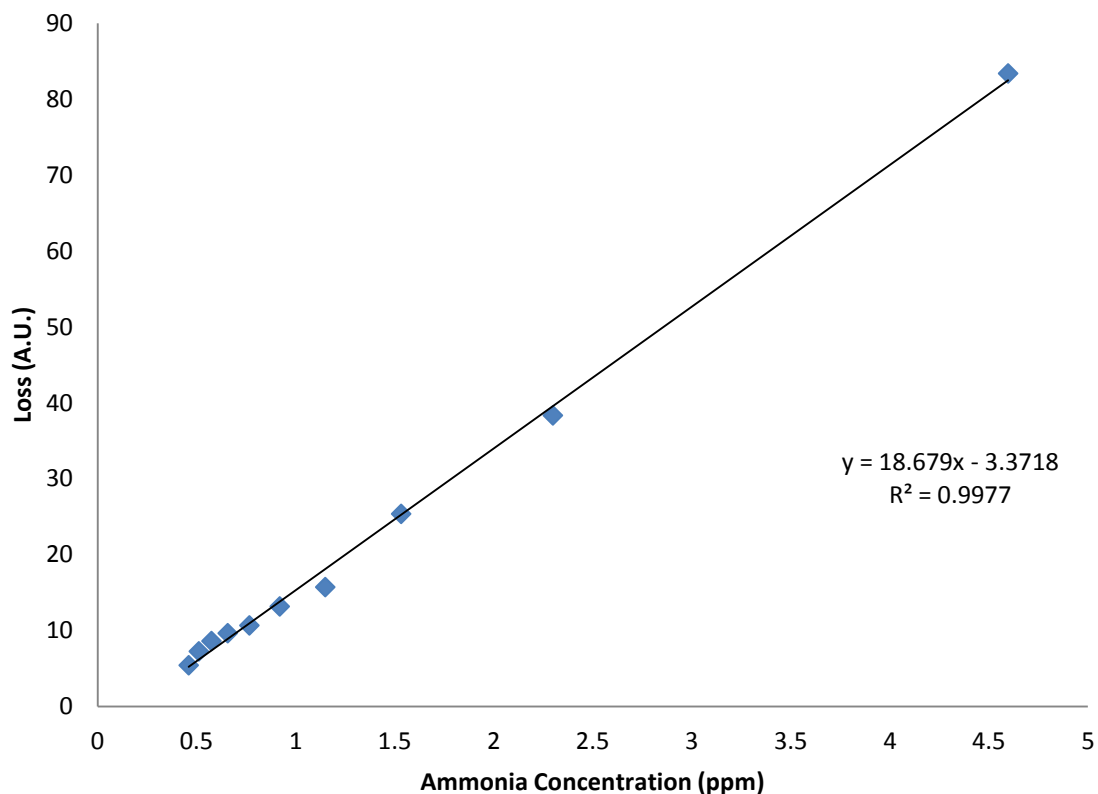


Fig. 7 Plot of measured ammonia absorption vs. concentration at one of the absorption maxima ( $930\text{ cm}^{-1}$ )

Plotting the measured loss versus the ammonia concentration reveals a linear relationship between the two. This linear relationship, depicted with a linear-fit trend line, allows for the calculation of the lowest detectable concentration of ammonia using a three sigma ( $3\sigma$ ) calculation. The  $3\sigma$  calculation is accomplished by dividing three times the standard deviation of the background by the slope of the linear fit.<sup>1</sup> Performing this calculation for the strongest ammonia absorption maxima, we determined the ammonia limit of detection to be 18.1 ppb for the LGR CRDS.

Analysis of the detection threshold depends on the studied chemical, and the recommended airborne exposure limit (REL) dictated by the National Institute for Occupational Safety and Health (NIOSH).<sup>17</sup> The REL for ammonia is 25 ppm averaged over a 10-h working day.<sup>17</sup> The

CRDS can measure ammonia concentrations that are well under the REL, and therefore, has met one of the most important design goals for the technology. That CRDS and the specific spectrometer analyzed at the US Army Research Laboratory (ARL) perform well for a specific compound does not imply that the performance can be extended for subsequent compounds. The methodology and spectrometers must be tested on further compounds of interest.

### 3.3 1,4-Dioxane

Evaluation of the second CRDS requires an analyte that fulfills the same two selection criteria that were used in the selection of ammonia. The second of the two spectrometers investigated is functionally identical to the first with one exception, the wavelength range of the excitation laser (1000 to 1240  $\text{cm}^{-1}$  or 8 to 10  $\mu\text{m}$ ). That means that ammonia cannot be used to evaluate the second spectrometer; another analyte must be chosen. The substance 1,4-dioxane has an absorption peak in the wavelength range of the second laser, and therefore, passes the binary first hurdle for selection. Also 1,4-dioxane fulfills the second of the selection criteria in that it is an analyte of interest in hazard detection that has immediate Army applications, given that 1,4-dioxane is a carcinogen, flammable, and possibly damaging to vital organs according to the New Jersey Department of Health and Senior Services.<sup>17</sup>

We followed the same recipe used previously with ammonia. We started with a high concentration of 1,4-dioxane and swept the excitation wavenumber, recording the spectrum of the analyte. Figure 8 is a plot of the measured loss versus wavenumber for the highest concentration of 1,4-dioxane. There are two clear absorption features, a small peak at 1053  $\text{cm}^{-1}$ , and a larger broader peak with three distinct maxima in the larger absorption envelop between 1104 and 1160  $\text{cm}^{-1}$ . The absorption maximum is at 1136  $\text{cm}^{-1}$  and that peak is used in the detection threshold calculations.

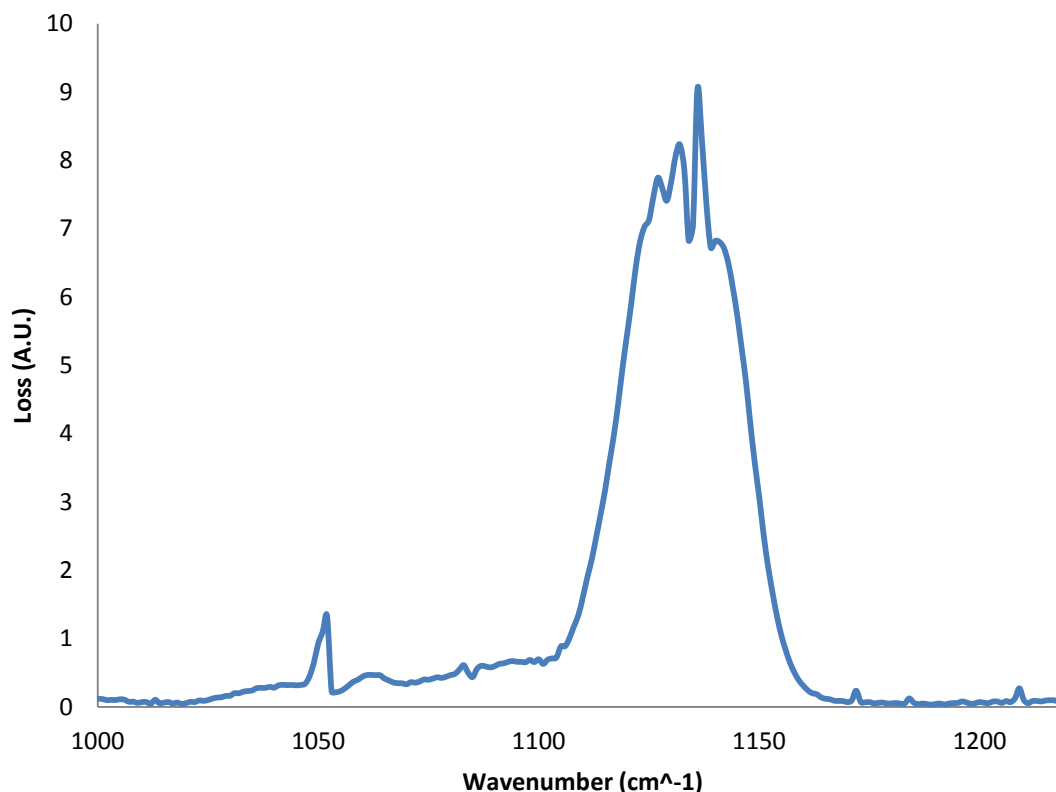


Fig. 8 Plot of loss vs. wavenumber for highest used concentration of 1,4-dioxane

There are clear absorption features in the investigated wavenumber range, just as in the ammonia spectra in Fig. 5, but the maximum loss measured for 1,4-dioxane is nearly an order of magnitude smaller than that of ammonia. This affects the limit of detection calculations that are made later in this report, as there is a lower SNR. Additionally, there are fewer points with which to compare the recorded 1,4-dioxane spectrum to a literature reference. Fewer peaks also make automated algorithm-based detection schemes more difficult. Despite those differences, the recorded behavior of the 1,4-dioxane spectra are more than adequate to showcase the capabilities of the spectrometer.

Beginning the limits of detection calculations starts again with evaluation of the changes in measured spectra as the analyte concentration varies. Plotting the spectra of 1,4-dioxane at varying concentrations on the same plot (Fig. 9) is a good way to see how decreasing analyte concentration lowers the measured signal. The overall shape of the plot remains constant, but the amplitude drops precipitously with the drop in concentration.

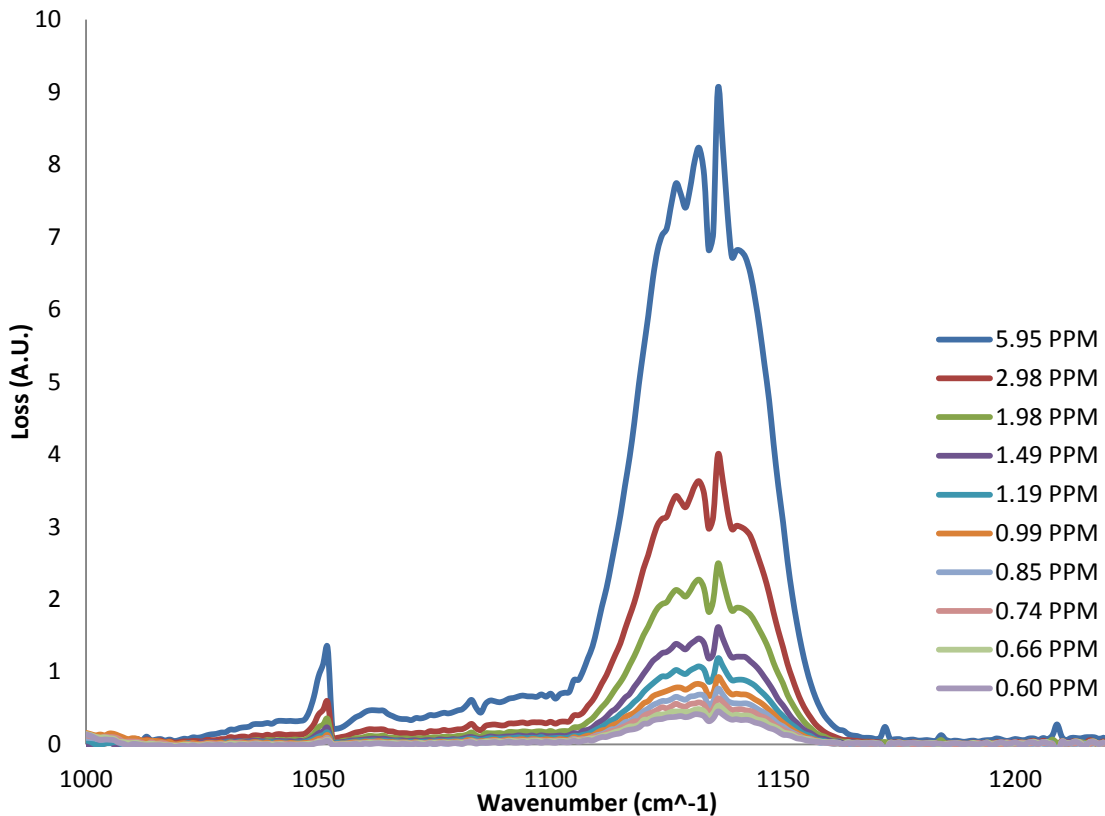


Fig. 9 Measured loss vs. excitation wavenumber for multiple 1,4-dioxane concentrations

It is obvious, when comparing Fig. 9 to Fig. 6, that the peak wavenumber for the absorption maximum does not fluctuate for 1,4-dioxane as much as it does for ammonia. This consistency is likely a result of the stability in the tuning of the second laser more so than environmental concerns. The decrease in peak wavelength fluctuations will increase the sensitivity of the spectrometer because the standard deviation of the background noise will be lower due to more stable experimental conditions. The next step in the limits of detection process is to examine the relationship between absorption maximum and concentration. Just as for ammonia, the relationship between those two factors is linear, as seen in Fig. 10.

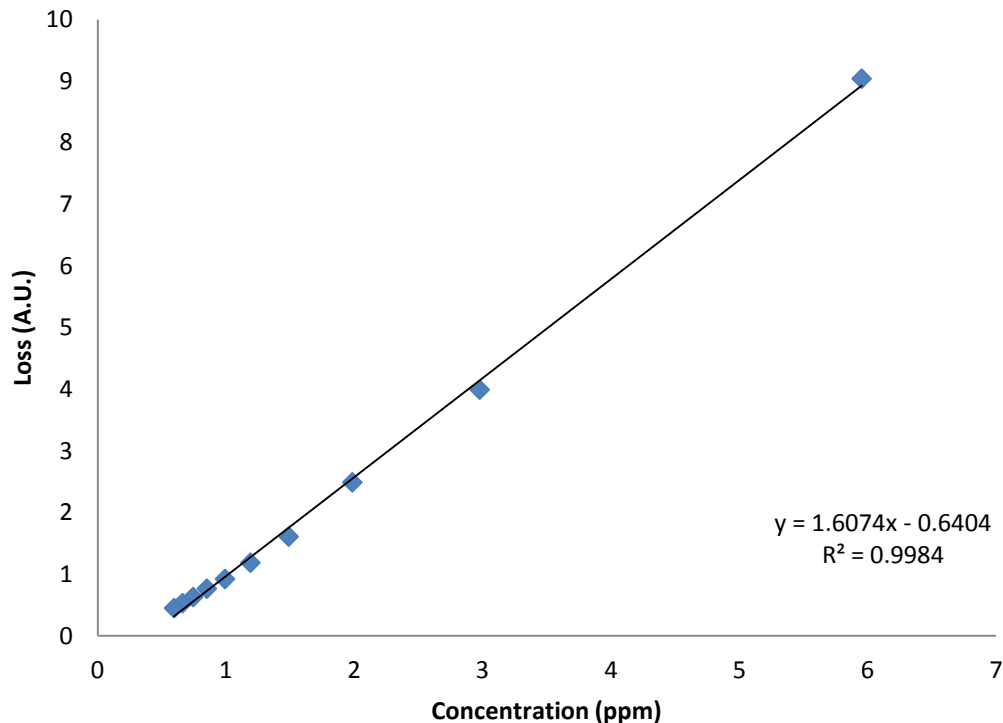


Fig. 10 Measured loss vs. 1,4-dioxane concentration

Following the same prescription from the limit of detection calculation for ammonia, the standard deviation of the measured nitrogen background for the second spectrometer was calculated.<sup>1</sup> Three times that value was divided by the slope of the linear fit from Fig. 10 to get the lower limit of detection for 1,4-dioxane. Calculations show that the lowest theoretical concentration of 1,4-dioxane that can be detected is 27 ppb. According to NIOSH, the REL for 1,4-dioxane is 1 ppm, not to be exceeded during any half-hour period.<sup>17</sup> This limit is well above the detection threshold for the spectrometer making it more than capable of detecting 1,4-dioxane well before harmful levels are present.

Comparisons between the calculated limits of detection for ammonia and 1,4-dioxane are excellent markers of experimental success. They show that the evaluated detectors are capable of meeting design specifications for hazard detection. However, evaluation of the spectrometers does not stop with limit of detection calculations. The chosen analytes have been studied numerous times before and those studies will serve as a baseline against which the experimental results are measured.

---

## 4. Literature Comparison

---

### 4.1 Public Databases

The data produced by the CRDSs must be analyzed against external sources. This comparison is done to remove experimental and instrumental bias and noise sources, and to analyze the utility and effectiveness of the spectrometers. The external sources range from massive online databases of infrared spectra<sup>18</sup> to data taken at ARL previously with other spectroscopic devices.<sup>19</sup> There are challenges associated with comparing data sets across multiple experimental platforms and databases. These challenges arise from comparing results of different experimental conditions and sensitivities.

Spectroscopic measurements, at their core, are relative measurements. It is more important to know the relative size of one absorption peak to another on the same spectrum, rather than knowing the absolute numerical value of that measurement. This emphasis on relative values can be seen in Section 3 where absorption values are plotted as functions of excitation wavenumber. The absorption value is reported in “A.U.”. Often an absorption spectrum will be normalized with the highest absorption peak value taking on an absorption value of one, and the rest of the spectrum being scaled accordingly. Normalization and arbitrary units makes qualitative comparison between spectra recorded under dissimilar conditions easier.

The two databases used for qualitative comparison of the measured spectra are from the National Institute of Standards and Technology (NIST)<sup>20</sup> and the Pacific Northwest National Laboratory (PNNL).<sup>21</sup> These databases consolidate spectroscopic information from a variety of sources and from measurements taken by the laboratory responsible for the database.<sup>18</sup> The PNNL data were collected onsite and come with information pertaining to the experimental conditions under which the data were collected. The NIST data come from a variety of sources and are available digitally as graphical data.

### 4.2 Ammonia

The different origins, formats, and experimental conditions under which the reference data were collected make a singular comparison infeasible. Instead, we examine each reference database against the experimentally generated CRDS. The PNNL data can be plotted on the same graph as the data collected with the CRDSs, whereas the NIST data, available online in graphical form, are compared as two separate images. The PNNL database has three data sets for ammonia, each recorded at different temperatures.<sup>22</sup> We use the PNNL spectrum, recorded at 25 °C, which is closest in temperature to the CRDS experimental data, recorded between 20 and 25 °C.

This spectrum is a small piece of the larger infrared absorption spectrum of ammonia available from PNNL. We select the portion of the PNNL data that coincides with the operating range of

the excitation laser in the CRDS. The features are much sharper in Fig. 11 than seen with the CRDS in Fig. 5. This is because the PNNL data have significantly higher spectral resolution, about 20 times finer, than the instruments from LGR. This high resolution allows for the large absorption feature between 920 and 940  $\text{cm}^{-1}$  to be seen as a collection of smaller peaks branching off from the main absorption peak at 930  $\text{cm}^{-1}$ . The difference in resolution is striking when we plot both the PNNL and CRDS ammonia data on the same plot (Fig. 12).

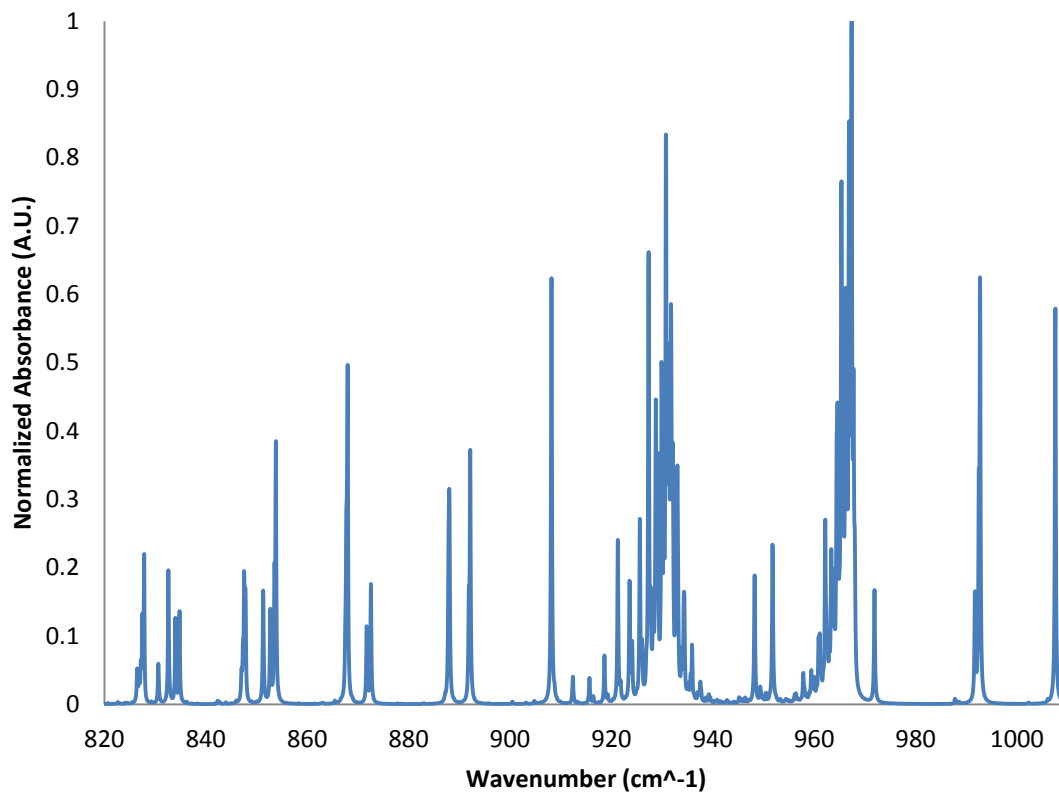


Fig. 11 Ammonia spectrum from PNNL

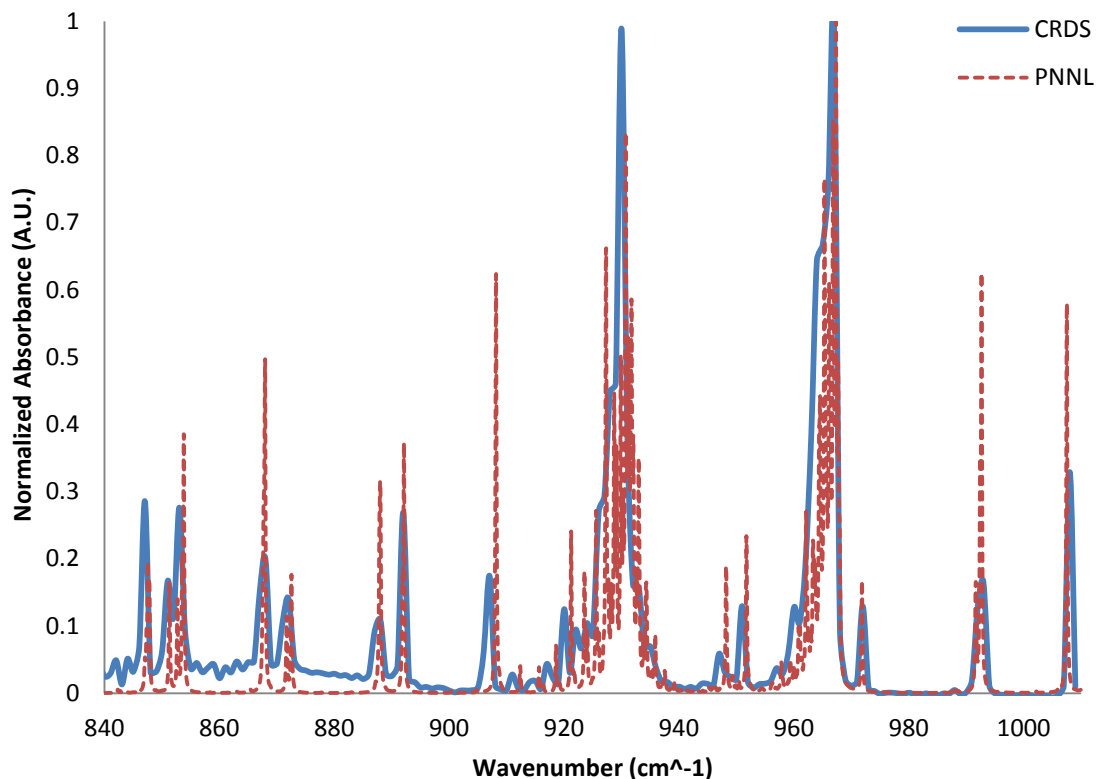


Fig.12 Comparison between CRDS (blue) and PNNL (red) absorption spectra for ammonia

The two spectra are very similar in terms of absorption peak placement and general shape, but it is clear that the PNNL data document more features than the CRDS data. The doublets discussed in Section 3.2 are still present, and many of the small fluctuations ( $<0.1$  A.U. absorbance) appear to be spectral features that both the CRDS and PNNL data sets capture. There are slight shifts the position of the spectral features between the two data sets, but not nearly as pronounced as the higher concentrations of ammonia. We know that the PNNL data were taken with an ammonia concentration of 1 ppm, and the spectral shifting seen above 2 ppm does not appear, which supports the molecular effect postulation from Section 3.2.<sup>15,16</sup> There are, however, differences between the two spectra. Several of the peaks have different relative sizes between the two spectra. Peaks at 908 and 992  $\text{cm}^{-1}$ , for example, are much larger relative to the rest of the spectrum for PNNL, and the peak at 930  $\text{cm}^{-1}$  is more dominant in the CRDS data set. This relative shifting of peak intensity is interesting, though less relevant in detection algorithms than peak location shifts. Overall, the equivalent concentration CRDS data are an excellent match for the PNNL data, and a solid check on the capabilities of the evaluated spectrometer.

The first of two NIST data sets for ammonia is from the Coblenz Society, and the data have been digitized from a hard copy of a spectra recorded in 1964.<sup>23</sup> This data set has a resolution of 4  $\text{cm}^{-1}$ , compared to a resolution of 1  $\text{cm}^{-1}$  in the experimental CRDS data and a 0.6  $\text{cm}^{-1}$  resolution for the PNNL data. Additionally, the imprecision of the reduced resolution also has

issues inherent in the digitization of graphical data. There are interpolated numerical data points available for this spectrum, but the uncertainty associated with the origins of the data limits the quantitative usefulness. Qualitatively, however, this data set, in addition to the second ammonia spectra from NIST, can be used to confirm the data recorded by the CRDSs. The second data set from NIST does not have chronological or formatting information available. The only information about the data set is that it is the result of an Environmental Protection Agency contract with Sadtler Research Labs.<sup>24</sup> There is also no concentration or resolution information available. The two NIST spectra are compared to two of the recorded ammonia spectra from the CRDS, as seen in Fig. 13.

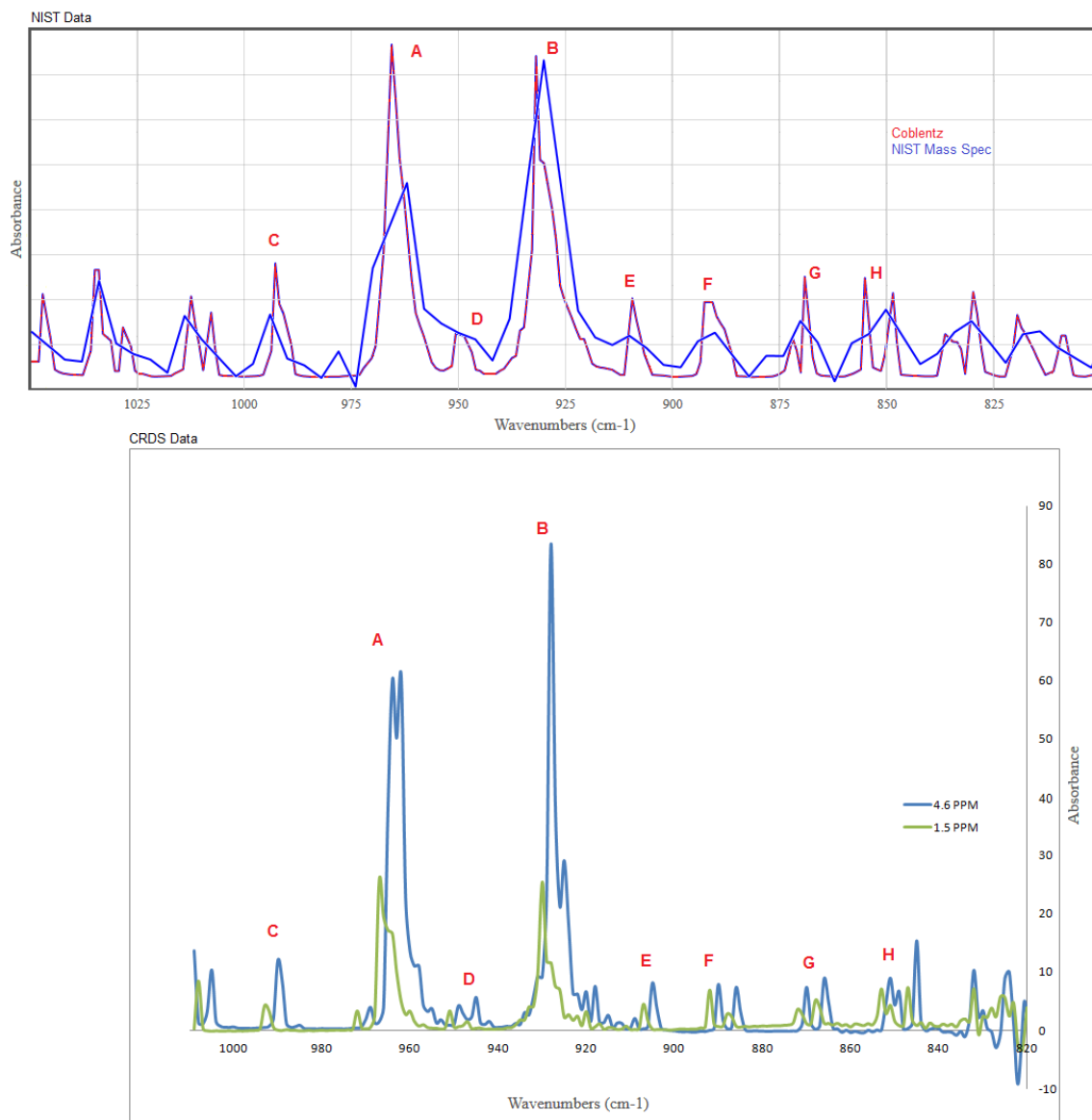


Fig. 13 Comparison of ammonia spectra from NIST (top) and CRDS (bottom). The letters A through H denote spectral features used for comparison between the four spectra.

The starting point for the analysis of the plots in Fig. 13, before comparing the NIST data sets to the experimental CRDS data, is the analysis of the two NIST spectra in the top plot. The red plot is the digitization of data from the Coblenz Society<sup>23</sup> and the blue spectrum is from the NIST Mass Spec Data Center.<sup>24</sup> The two spectra agree with each other in terms of general shape and spectral feature locations. The two spectra have two main absorption maxima, A and B, and several minor features C through H. The relative size difference between the maxima and the minor features is the same between the two data sets. However, it is clear that the data sets differ in key areas. The first key difference between the two NIST spectra is that the NIST Mass Spec data have a much lower resolution than the  $4\text{ cm}^{-1}$  reported for the Coblenz Society data. The lack of resolution leads to the obfuscation of spectral features. What were clear absorption doublets in spectral features F, G, and H, discussed in Section 3.2, are now seen as single absorption peaks. Additionally, several secondary and tertiary peaks are absent from the spectrum. The example of a secondary peak near the apex of maxima B can be seen in the higher resolution Coblenz data, but not in the NIST Mass Spec data. Though the two data sets have different resolutions, they are both important in the overall analysis of the ammonia data. Another important difference between the two spectra is the slight but noticeable shift in the absorption maxima, features A and B. The maxima in the NIST Mass Spec data are located at slightly lower wavenumbers than the corresponding maxima in the Coblenz data. Additionally, the relative size of the two maxima is different between the two data sets.

The reference data from NIST have several important similarities with the measured CRDS data. The first is the illustration that different spectra of ammonia can have different relative peak sizes, shapes, or locations without the spectra losing their overall picture of ammonia absorption. It is clear that some of the differences between the two CRDS spectra in the bottom plot of Fig. 13 are not artifacts of the CRDS, as they also appear in the NIST reference data. Mutability of peak dominance between maxima A and B shows up, as does the slight shift in peak wavelength absorption. It might be interesting to note that the shift in wavenumber and the swapping of relative absorption maxima occur in tandem, i.e., the Coblenz data and the 1.5-ppm data appear to be analogous in that regard, and the same with the NIST Mass Spec data and the 4.6-ppm data. However, the similarity might merely be a coincidence of having few data sets, and further examination of data might show that the two shifts occur separately. The lack of concentration information from the NIST data sets prohibits the possible confirmation of the molecular interactions thought to be responsible for the shifting peak wavelength values. Overall, the comparison between the NIST data sets, the data from PNNL, and the experimentally produced data from the CRDS spectrometer show excellent agreement, certainly enough to verify that the experimental data are within desired tolerances for accuracy.

### **4.3 1,4-Dioxane**

Verification of the second CRDS necessitated the use of a second analyte with active absorption features in the wavenumber range of the QCL. As such, 1,4-dioxane, discussed in Section 3.3, fit the specifications of spectral activity and hazardous interest for the Army. The comparison of

experimental 1,4-dioxane spectra to reference data starts with the analysis of the spectrum referenced from PNNL, seen in Fig. 14. Like the ammonia data from PNNL, the 1,4-dioxane spectrum was recorded at 25 °C with an analyte concentration of 1 ppm.

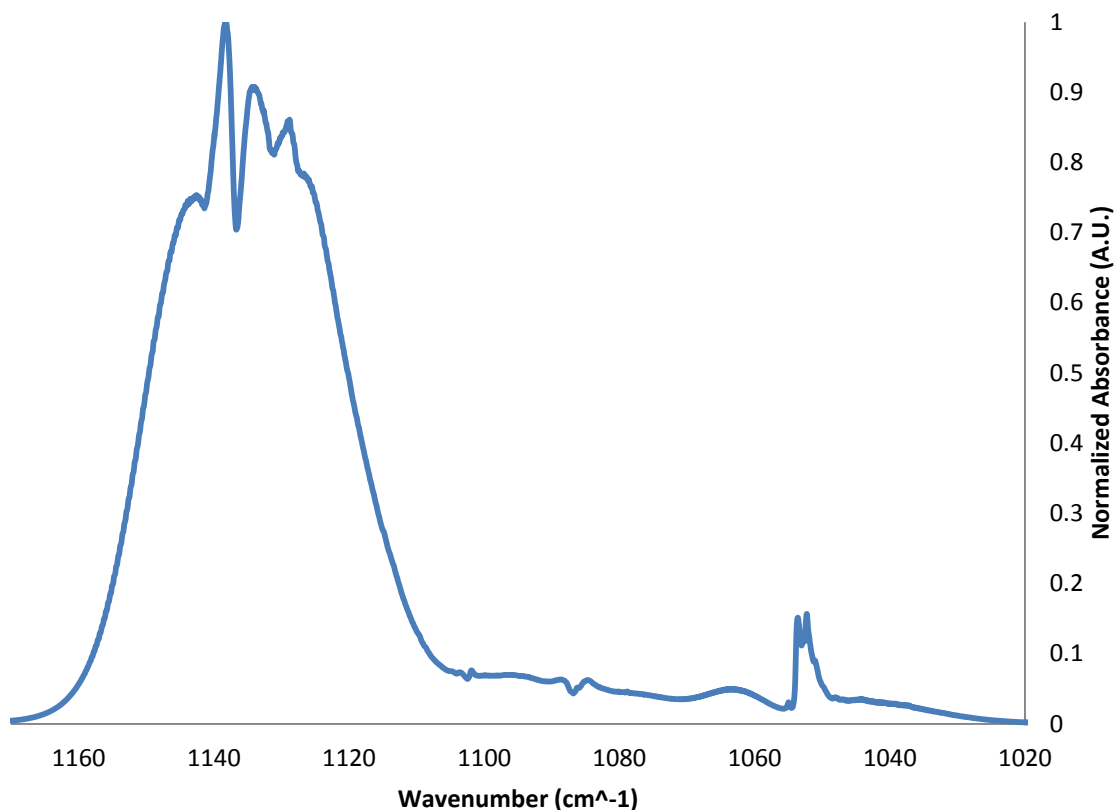


Fig. 14 1,4-dioxane spectrum from PNNL

There are two slight differences in the presentation of the 1,4-dioxane data that show up in Fig. 14 and in the proceeding plots. The first is that the  $x$ -axis of the plot has been reversed to show wavenumbers in decreasing order. This is done for consistency with reference data presentation. Additionally, the range of the  $x$ -axis has been truncated to magnify the two spectral features that are used in the comparative analysis of the experimental data. This truncation does not eliminate any important information. There are two primary spectral features that are discussed from Fig. 14. There is a small absorption peak at  $1053\text{ cm}^{-1}$ , and a  $60\text{ cm}^{-1}$  wide absorption maximum between  $1160$  and  $1100\text{ cm}^{-1}$ . Inside of that wider absorption maximum, there are distinct peaks, the local maximum, and global maximum for the wavelength range of interest, which is located at  $1138\text{ cm}^{-1}$ .

The plot of the normalized 1,4-dioxane spectra from PNNL and the CRDS is in nearly perfect alignment. The two separate spectra in Fig.15 are almost hard to differentiate, with the only minor difference being the secondary peak at  $1052\text{ cm}^{-1}$  in the PNNL data that does not appear in the CRDS data. That minor difference between the two spectra is a factor of the significantly

increased resolution available in the PNNL data. The other spectral features are broad enough that the CRDS is capable of sufficiently resolving them.

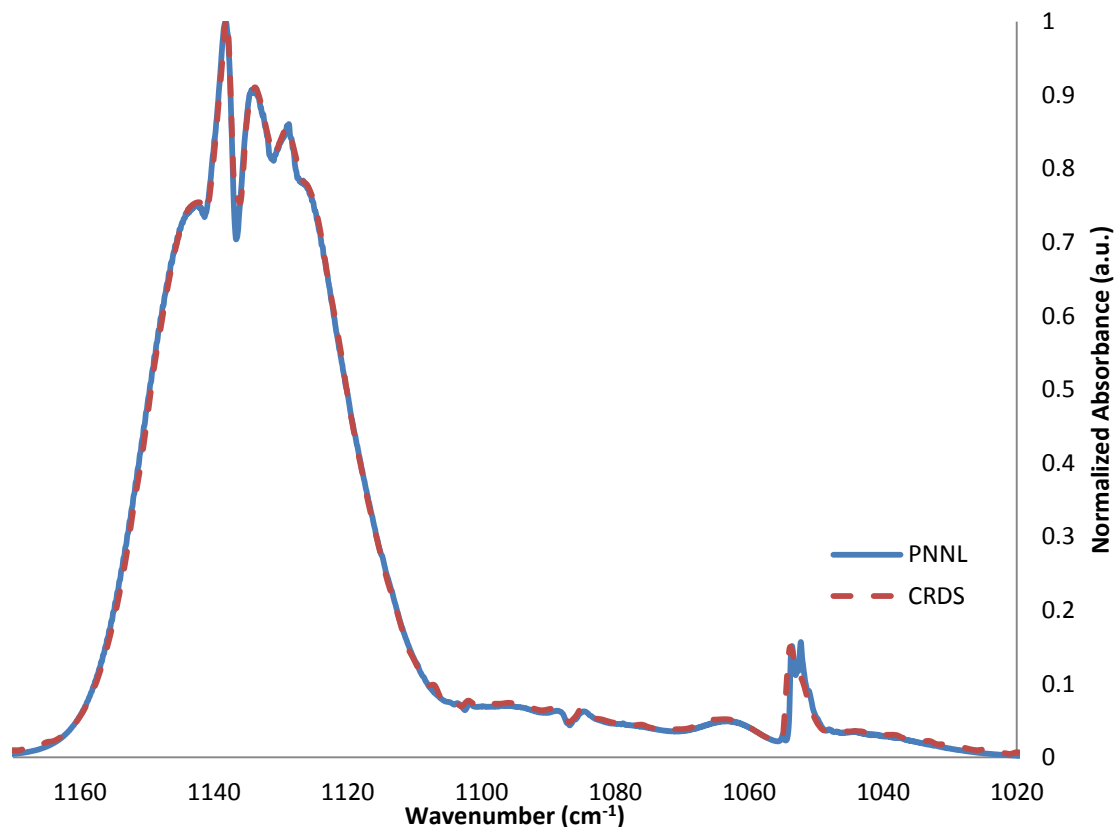


Fig. 15 Comparison between PNNL (blue) and CRDS (red) spectra for 1,4-dioxane

The overlap of the two spectra did not occur natively with the raw CRDS data. There is a constant  $2\text{ cm}^{-1}$  wavenumber shift applied to the domain of the CRDS data. This shift is not caused by the same molecular effects that shifted the spectrum of ammonia; instead, it is a product of the excitation laser used in the spectrometer. The shift is likely due to a simple calibration error within the excitation laser and does not affect the effectiveness of the spectrometer. The agreement between experimental and reference data in Fig. 15 provides a clear picture of the capabilities of the CRDS. Further comparison to NIST reference data confirms this.

There are four data sets of 1,4-dioxane spectra available for reference from the NIST database. Three of the spectra are from the Coblentz Society<sup>23</sup> and the remaining spectrum is from the NIST Mass Spec Data Center.<sup>24</sup> We compared the two most useful spectra from the NIST electronic database, one from each source. The two spectra in Fig. 16 are quite similar to each other and have the same basic shape that can be used to identify 1,4-dioxane. The blue spectrum, from the NIST Mass Spec Data Center, does not have the same level of detail as the red spectrum from the Coblentz Society. It is clear that the absorption maximum in the red spectrum

is not a broad, smooth peak. There are three different features that can be identified at the apex. Those features have been identified with the letters A through C and the smaller side peak at the low wavenumber end of the spectrum in both reference spectra is denoted D. Comparison of the reference data to the CRDS data shows a clear match between them. The wavenumber resolution for the experimental data is much higher than that of the NIST reference, leading to more distinction between features A through C, even when the SNR is lower for the lower concentration green spectral line.

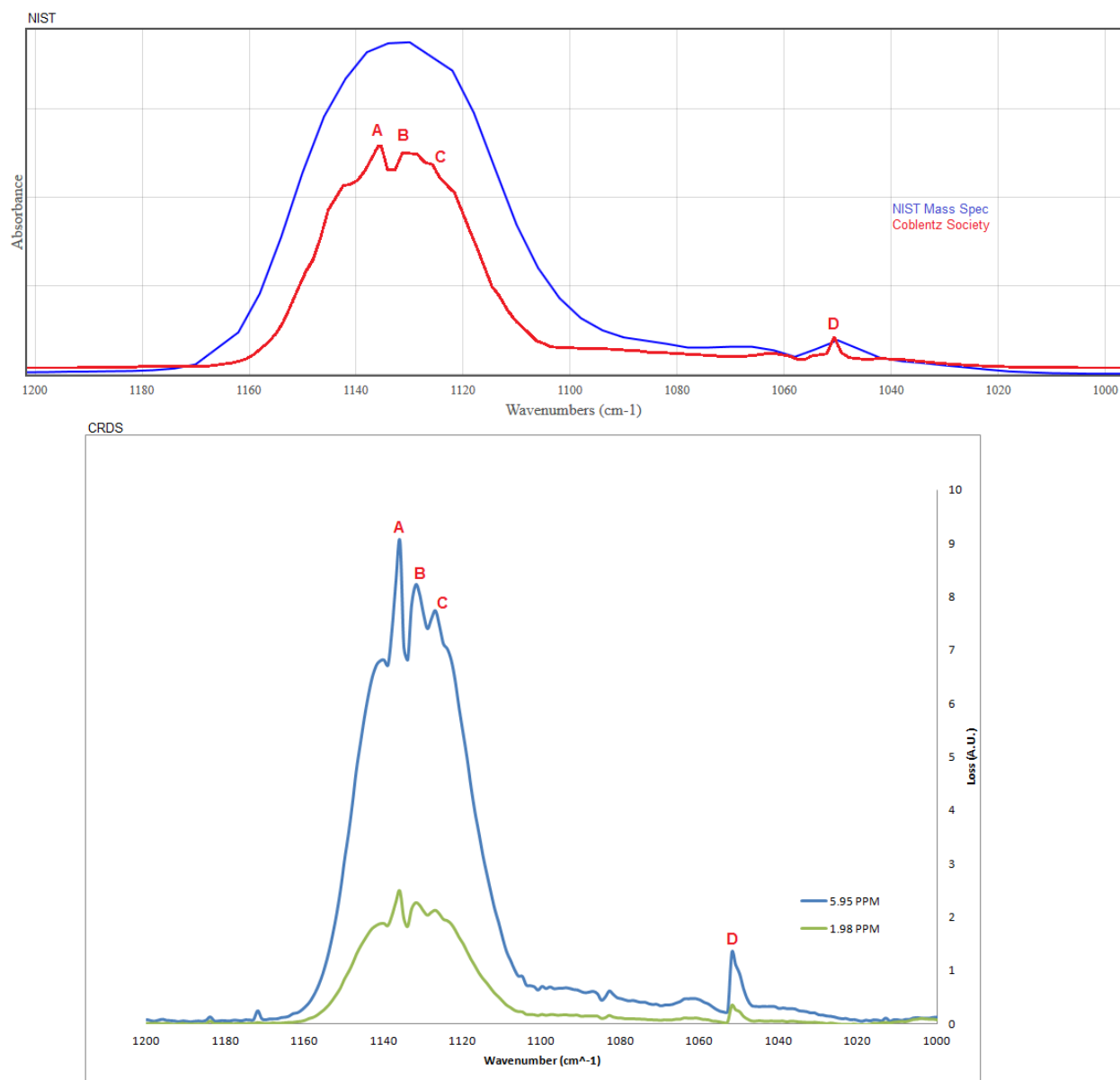


Fig. 16 Comparison between NIST reference data (top) and CRDS experimental data (bottom). The two spectra in the top plot have different data sources and sensitivities.

The comparisons between the two reference databases, NIST and PNNL, show that the CRDS is capable of accurately measuring the infrared absorption spectra of the two selected analytes. While it would be hasty to say that the spectrometers could be used to measure any analyte, it is not too much of a stretch to say with some certainty that analytes with absorption features in the wavelength range of the two excitation lasers could be measured accurately.

#### **4.4 ARL Experimental Data Comparison**

The Optical Devices and Sensors (ODS) team in the Sensors and Electron Devices Directorate (SEDD) of ARL was chosen as a natural collaborator with ECBC because of their extensive experience in spectroscopy. This experience aided the experimental setup and execution, as all the required materials were in place, including the two studied analytes. Furthermore, the previous experimental results in infrared spectroscopy obtained by the ODS team can be used as another reference point for the CRDS data. The internally generated ARL data come from two different spectroscopic methods, PAS and FTIR. The PAS data were taken using the experimental setup developed at ARL.<sup>19</sup> The FTIR data were taken using a Nicolet 6700 FTIR spectrometer (Thermo Scientific). Those methods have been used to measure the infrared absorption spectrum of 1,4-dioxane in a similar wavelength range to that of the CRDS experiment.

The comparison between internally generated ARL reference data in the CRDS data serves as the last check on the capabilities of the spectrometers. The experimental data used in this comparison have the advantage over the electronic database data in that they come from a source where the parameters of the data acquisition are well known. The PAS data have a wavenumber resolution of  $1\text{ cm}^{-1}$ , matching the resolution of the CRDSs. The resolution of the FTIR data is twice that of the other two methodologies at  $\frac{1}{2}\text{ cm}^{-1}$ . We are able to examine the data all on the same plot because the raw data are available for the PAS and FTIR spectra. This comparison can be done with normalized data sets with the normalization accomplished by setting the value of the maximum signal to unity and adjusting the rest of the data proportionally. There are four data sets for three different spectroscopic methods, as shown in Fig. 17. The two CRDS spectra are from the concentrations used throughout Section 3: 5.96 ppm (green) and 1.98 ppm (black). The FTIR data, discussed above, are in red and the PAS data are in blue.

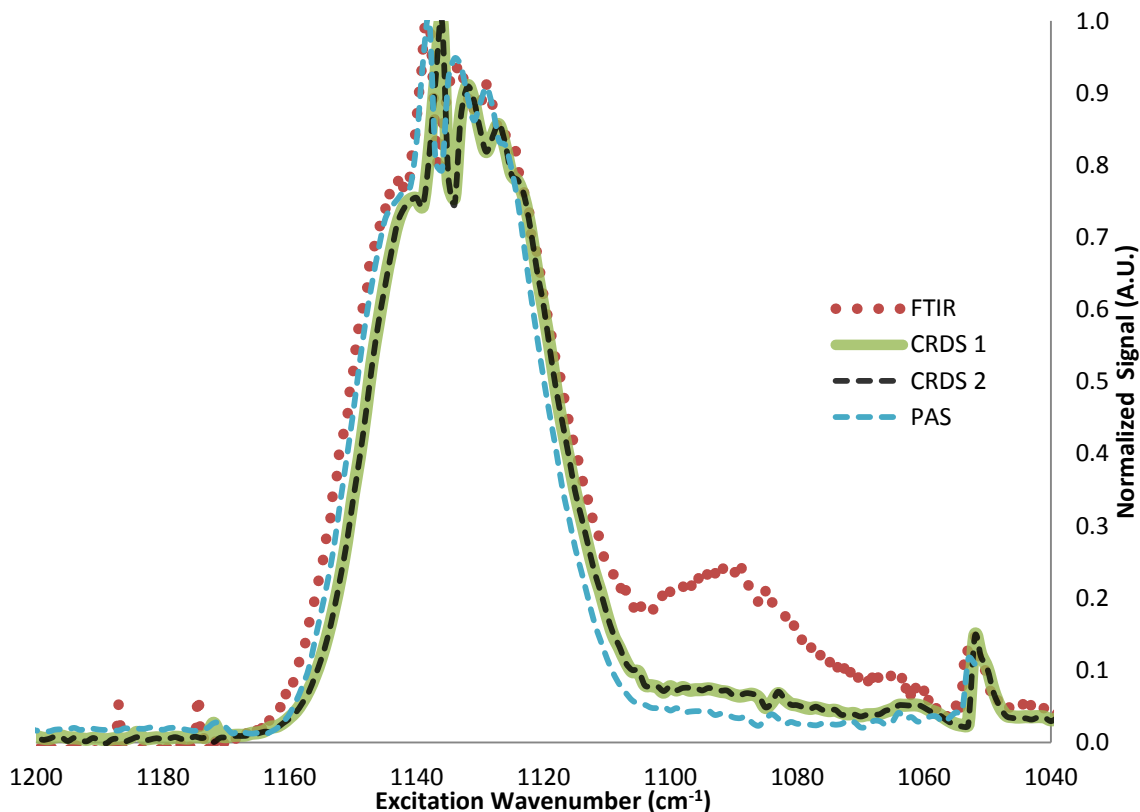


Fig. 17 Comparison of the three spectroscopic methods. The two CRDS spectra (green and black) are compared to FTIR (red) and PAS (blue).

A first coarse look shows excellent agreement on the main spectroscopic features. There are four main features that were examined in the previous section when comparing the CRDS data to the available reference databases. Those four points, A through D in previous discussions, are the three peaks inside of the local absorption maximum and the smaller peak located at around  $1050\text{ cm}^{-1}$ . Those points are all visible in all four spectra, though there is a clear downshift in their wavenumber when going from the FTIR and PAS data to the CRDS data. This shift looks like a constant translation of the spectrum of the same number of wavenumbers, and thus, is likely due to a systematic difference in laser tuning or calibration. The consistency of this translation difference does not affect the viability of the CRDS technology as it is something further calibration would likely eliminate. Once the linear shift in wavenumbers is compensated for, the spectra align almost identically.

This is final confirmation of the ability of the CRDSs to accurately reproduce chemical spectra for the species tested and evaluated by the ODS team at ARL. The technology must be extensively evaluated for each new chemical species it will be used to detect, but without loss of generality, it can be seen that the CRDSs will work for chemical species with absorption features in their wavelength ranges.

---

## 5. Conclusions

---

The goal of the collaboration between ARL and ECBC was the evaluation of a pair of CRDSs delivered to the US Government by LGR as part of a SBIR. The evaluation has focused on the reproduction of infrared absorption spectra for hazardous reference materials that are of immediate interest to the health and safety of the US Army. The two chosen analytes, ammonia and 1,4-dioxane, are both hazardous materials as defined by NIOSH and other Government agencies.<sup>17</sup> The spectra produced by the CRDSs have been evaluated for accuracy against both external and internal reference data, and for utility against Governmental safety standards.

Accurate re-creation of accepted reference spectra is one of the main evaluation criteria used when examining a new spectroscopic device. The CRDSs described herein were shown to faithfully reproduce the reference spectra from two different databases maintained by national laboratories. It is clear that the experimental data from the CRDSs are measuring the same unique identifying features for the two analytes tested. Further analysis of internal data from different spectroscopic methodologies confirmed the accuracy of the LGR products.

The examined internal ARL data were helpful in confirming spectral features observed in the CRDS spectra. These data do not have the same status as the external databases, but are crucial nonetheless in the analysis process. We had tighter control over the experimental parameters of the internally generated data and complete information of the generation of the data. This allows for the identification of possible systemic issues in the internal data and for the confirmation of the experimental results of the CRDS. A slight shift in the wavenumber of the absorption peaks is one such feature that the internal data were able to identify. Though this is a negligible shift as far as the performance of the spectrometers are concerned, knowledge of the shift would allow for compensation if deemed necessary.

The goal of this study was not to determine the best infrared absorption spectroscopy method for the Army; it was to examine and evaluate two specific devices that were designed to measure infrared spectra. The strengths and limitations of the CRDS method are important, however, to the conversation about the LGR spectrometers as spectroscopic tools. Perhaps the most important feature of the CRDS method is the elongated effective path length that the laser pulse has to interact with the analyte. This feature is incredibly important to concentration studies, and the LGR spectrometers proved to be up to the desired task of measuring sub-dangerous levels of the chosen analytes. The instruments performed well for the purpose of early warning or trace detection of hazards, with detection limits in excess of 30 times smaller than hazardous levels of the studied analytes. The excitation lasers inside of the spectrometers are both broadly tuned and commercially produced. The broad tuning of the excitation source allows for multiple analytes to be investigated for one source, and the commercial origin of the laser means that the spectrometers can be upgraded as the QCLs are.

There are drawbacks to the examined spectrometers that might limit their utility. The first is that the device requires a carefully aligned optical setup to minimize the detection threshold. The excitation laser must be injected into the cavity in such a way as to maximize the path length of the laser pulse. The mirrors that truncate each end of the cavity must also be carefully aligned to maximize the effectiveness of the spectrometers. There is a critical need for optical stability limits on where and how the spectrometers are used. The second main limitation of the system is the liquid nitrogen cooled HgCdTe detector. That the detector needs a steady supply of liquid nitrogen as coolant severely limits the environments in which the detectors are useful and hampers the portability of the system. Some of the problems associated with the CRDSs are endemic to infrared spectrometers, including analyte delivery and overall device size. The spectrometers as analyzed do not have any way of collecting ambient gaseous samples for analysis, thus the need for external gas supply equipment. The size of the spectrometers, roughly 5 ft<sup>3</sup>, is not ideal for all applications, but that is a problem shared by most other spectroscopic methods. However, the sample chamber used by the CRDSs is much larger than the equivalent for PAS or FTIR methods. The engineering solutions for the aforementioned drawbacks are beyond the scope of this report, and the drawbacks themselves are minor when compared to the previously discussed success of the spectrometers.

Future work on CRDS would include possible engineering solutions to the minor drawbacks of the CRDS method, including ruggedizing the spectrometer and finding a more efficient way of cooling the detector. Work must also be done to generate a spectral library of airborne threats so that detection and identification of airborne hazards can be accomplished. Further work including detector optimization and miniaturization of system components should be considered as well.

Overall, the CRDS systems evaluated by ARL performed admirably with respect to the detection of trace levels of hazardous gaseous analytes. CRDS has a unique advantage over other infrared spectroscopy methods: the interaction path length for the excitation pulse in a CRDS experiment is on the order of 10 km. This advantage differentiates CRDS from other methodologies and allowed for the low limits of detection for the hazardous analytes discussed previously. CRDS technology is a method that should be further investigated for the needs of the US Army for airborne hazard detection.

---

## 6. References

---

1. Holthoff EL, Heaps DA, Pellegrino PM. Development of a MEMS-scale photoacoustic chemical sensor using a quantum cascade laser. *IEEE Sensors J.* 2010;10(3):572–577.
2. Wheeler MD, Newman SM, Orr-Ewing AJ, Ashfold MNR. Cavity ring-down spectroscopy. *J Chem Soc, Faraday Transactions.* 1998;94(3):337–357.
3. Skoog DA, West DM. *Principles of instrumental analysis*, 2 ed. Philadelphia (PA): Saunders College; 1980.
4. Larkin PJ. *IR and raman spectroscopy*. New York (NY): Elsevier; 2011.
5. O'Keefe A, Deacon DAG. Cavity ringdown optical spectrometer for absorption measurements using pulsed laser sources. *Rev Scientific Instruments.* 1988;59:2544–2551.
6. Jacquet P, Pailloux A, Aoust G, Jeannot J-P, Doizi D. Cavity ring-down spectroscopy for gaseous fission products trace measurements in sodium fast reactors. *IEEE Transactions on Nuclear Science PP.* 2014;(99):1.
7. Berden G, Peeters R, Meijer G. Cavity ring-down spectroscopy: experimental schemes and applications. *Intl Rev Physical Chem.* 2000;19(4):565–607.
8. Romanini D, Lehmann KK. Ringdown cavity absorption spectroscopy of the very weak HCN overtone bands with six, seven, and eight stretching quanta. *J Chem Physics.* 1993;99(9):6287–6301.
9. Harris DC. *Quantitative Chemical Analysis*. New York (NJ): W. H. Freeman and Company; 1999.
10. Los Gatos Resarch, Inc. January 13, 2014. Available: <http://www.lgrinc.com/about/about.php>
11. Daylight Solutions, Inc. 14 January, 2014. Available: <http://www.daylightsolutions.com>
12. Owlstone Nanotech, Inc. 15 January, 2014. Available: <http://www.owlstonenanotech.com/company>
13. Occupational Safety and Health Administration. 21 January, 2014. Available: <https://www.osha.gov/SLTC/emergencypreparedness/guides/chemical.html>
14. McKean DC, Schatz PN. Absolute infrared intensities of vibration bands in ammonia and phosphine. *J Chem Physics.* 1956;24(2):316–325.

15. Suzer S, Andrews L. FTIR spectra of ammonia clusters in noble gas matrices. *J Chem Physics* 1987;87(9):5131–5140.
16. Firanescu G, Luckhaus D, Signorell R. Size effects in the infrared spectra of NH<sub>3</sub> ice nanoparticles studied by a combined molecular dynamics and vibrational exciton approach. *J Chem Physics*. 2006;125:144501.
17. State of New Jersey Department of Health. 22 January, 2014. Right to Know Hazardous Substance Fact Sheets. Available:  
<http://web.doh.state.nj.us/rtkhsfs/factsheets.aspx?lan=english&alph=A&carcinogen=False&new=False>
18. Sharpe SW, Johnson TJ, Sams RL, Chu PM, Rhoderick GC, Johnson PA. Gas-phase databases for quantitative infrared spectroscopy. *Applied Spectroscopy*. 2004;58(12):1452–1461.
19. Holthoff E, Bender J, Pellegrino P, Fisher A. Quantum cascade laser-based photoacoustic spectroscopy for trace vapor detection and molecular discrimination. *Sensors*. 2010;10:1986–2002.
20. National Institute of Standards and Technology. 28 January, 2014. Available:  
<http://www.nist.gov>
21. Pacific Northwest National Laboratory. 29 January, 2014. Available: <http://www.pnl.gov>
22. Pacific Northwest National Laboratory. 14 January, 2014. Northwest-infrared vapor phase infrared spectral library. Available:  
<https://secure2.pnl.gov/nsd/NSD.nsf/Welcome?OpenForm>
23. Coblenz Society, Inc. 20 December, 2013. Evaluated Infrared Reference Spectra. Available:  
<http://webbook.nist.gov>
24. NIST Mass Spec Data Center. 30 January, 2014. Infrared Spectra. Available:  
<http://webbook.nist.gov>

---

## List of Symbols, Abbreviations, and Acronyms

---

$\alpha$	absorption coefficient
ARL	US Army Research Laboratory
A.U.	arbitrary units
$c$	speed of light
$\text{cm}^{-1}$	Inverse centimeter
CRDS	cavity ring-down spectroscopy/spectrometer
$e$	number $e$
ECBS	Edgewood Chemical Biological Center
ECQCL	external cavity quantum cascade laser
FTIR	Fourier transform infrared spectroscopy
HgCdTe	mercury, cadmium, tellurium
$I$	absorbed light intensity
$I_0$	initial light intensity
$l$	light travel distance
$L$	loss factor for end mirrors
LGR	Los Gatos Research, Inc.
$N$	number of round trips
NIOSH	National Institute for Occupational Safety and Health
NIST	National Institute of Standards and Technology
ODS	Optical Devices and Sensors Team
OSHA	Occupational Safety and Health Administration
PAS	photoacoustic spectroscopy
PMT	photomultiplier tube
PNNL	Pacific Northwest National Laboratory

PVD	photovoltaic detector
QCL	quantum cascade laser
R	reflectivity of end mirrors
REL	recommended airborne exposure limit
$\sigma$	standard deviation
SBIR	Small Business Innovation Research
SEDD	Sensors and Electron Devices Directorate
SNR	signal-to-noise-ratio
T	fraction of light transmitted through mirrors
t	time
$\tau$	empty cavity decay time
TIC	toxic industrial chemical

1 DEFENSE TECHNICAL  
(PDF) INFORMATION CTR  
only) DTIC OCA

2 DIRECTOR  
(PDF) US ARMY RESEARCH LAB  
RDRL CIO LL  
IMAL HRA

1 GOVT PRNTG OFC  
(PDF) A MALHOTRA

5 DIRECTOR  
(PDF) US ARMY RESEARCH LAB  
1 RDRL SEE E

(HC) PAUL M PELLEGRINO  
LOGAN S MARCUS (1 HC, PDF)  
ELLEN L HOLTHOFF  
GARY WOOD  
LINDA BLISS

3 EDGEWOOD CHEMICAL BIOLOGICAL CENTER  
(PDF) RDCB-DRD-P  
ALAN C SAMUELS  
ERIN D DAVIS  
ANGELA M BUONAUGURIO

INTENTIONALLY LEFT BLANK.